Contribution from the Department of Chemistry, University of California, Davis, California 95616,
and Department of Molecular Biology, Research Institute of Scripps Clinic, La Jolla, California 92037

Comparison of the Electronic Structures of Chromate, Halochromates, and Chromyl Halides by the Xα Method

R. M. Miller,[†] D. S. Tinti,*[,†] and D. A. Case[‡]

Received August 26, 1988

The electronic structures of CrO_4^{2-}, CrO_3X^-, and CrO_2X_2 with X = F and Cl are compared by using the SCF Xα–SW method. Results are presented for the ground state and for the lower lying singlet and triplet excitations. The lowest energy excited states are calculated to arise from the promotions $1t_1 \rightarrow 2e$ in CrO_4^{2-}, $1a_2 \rightarrow 9e$ in CrO_3F^-, $1a_2 \rightarrow 10e$ in CrO_3Cl^-, $7b_2 \rightarrow 14a_1$ in CrO_2F_2, and $8b_2 \rightarrow 17a_1$ in CrO_2Cl_2. The predicted energies and symmetries of the lowest lying excited states and their very small singlet–triplet splittings are in satisfactory agreement with the available experimental data for the halogen-substituted systems. Relativistic calculations for the ground state of CrO_4^{2-} suggest that spin–orbit interactions are not important for a qualitative description of the lower excited states.

Introduction

Since the initial studies of Wolfsberg and Helmholtz,[1] the electronic structures of tetraoxo complexes of closed-shell transition metals have received extensive theoretical investigation.[2-10] Much of this work has focused on MnO_4^-, as the archetypical complex, with other systems receiving less attention. Perturbation of the electronic structure engendered by changing one or more of the oxygen ligands for a given metal has received even less study. Recently, the lower excited states of CrO_4^{2-}, CrO_3X^-, and CrO_2X_2 with X = F and Cl have received renewed experimental interest with the observation of their previously elusive lowest lying spin-triplet states.[11-17] Prompted by these experimental results, the present theoretical study on this series of Cr(VI) complexes was undertaken to compare the electronic structure of the members of the series in a common calculational scheme. The Xα–scattered wave method, which has been reviewed by several authors,[5,18-20] is employed.

Computational Details

The point group symmetries were taken as T_d for CrO_4^{2-}, C_{3v} for CrO_3X^- and C_{2v} for CrO_2X_2 (X = F and Cl). The coordinate systems are defined by the atomic positions given in Table I. These were calculated from reported X-ray or electron diffraction results[21-25] with assumed tetrahedral angles for CrO_3F^-.

The relevant parameters for the present calculations are given in Table II. The atomic exchange parameters, α values, were taken from Schwarz,[26] and a valence-electron-weighted average of the atomic values was used for α in both the interatomic and outer regions. The atomic sphere radii were chosen by the Norman[27] criterion, which provides for some overlap, with the outer-sphere radius reduced from tangency with the most distant atomic sphere by 0.10 bohr. A Watson[28] sphere of positive charge with a radius equal to the outer sphere was used with the anions. The reported results employed an angular basis set with l_{max} equal to 4 for the outer shell, 3 for Cr and Cl, and 2 for O and F. Various calculations using a smaller angular basis did not yield any significant differences. The core levels (Cr 1s, 2s, 2p; O 1s; F 1s; Cl 1s, 2s, 2p) were included in the SCF procedure as single-atom functions.

Spin-restricted and spin-unrestricted (polarized) calculations were performed for the ground states and for the lower lying excitations. The excited-state energies were estimated by using orbital energies from transition-state calculations with half-integral occupation numbers for the relevant orbitals and by using the total statistical energies from calculations with integral occupation numbers for these orbitals. Relativistic Dirac scattered-wave calculations[20] for the ground state of CrO_4^{2-} used parameters identical with those for the nonrelativistic calculations.

Table I. Atomic Positions (in bohr)[a]

		x	*y*	*z*
CrO_4^{2-}	Cr	0.0000	0.0000	0.0000
	O	−1.8002	1.8002	1.8002
	O	1.8002	−1.8002	1.8002
	O	1.8002	1.8002	−1.8002
	O	−1.8002	−1.8002	−1.8002
CrO_3F^-	Cr	0.0000	0.0000	−0.0984
	O	−2.8430	0.0000	−1.1044
	O	1.4215	−2.4620	−1.1044
	O	1.4215	2.4620	−1.1044
	F	0.0000	0.0000	3.2076
CrO_3Cl^-	Cr	0.0000	0.0000	−0.7317
	O	−2.8721	0.0000	−1.6808
	O	1.4361	−2.4872	−1.6808
	O	1.4361	2.4872	−1.6808
	Cl	0.0000	0.0000	3.4057
CrO_2F_2	Cr	0.0000	0.0000	−0.0810
	O	0.0000	−2.4049	−1.8347
	O	0.0000	2.4049	−1.8347
	F	2.6931	0.0000	1.7389
	F	−2.6931	0.0000	1.7389
CrO_2Cl_2	Cr	0.0000	0.0000	−0.6374
	O	0.0000	−2.4247	−2.3830
	O	0.0000	2.4247	−2.3830
	Cl	3.3560	0.0000	1.5713
	Cl	−3.3560	0.0000	1.5713

[a] 1 bohr = 5.29177×10^{-11} m.

Table II. Sphere Radii (in bohr)[a] and α Exchange Parameters

	CrO_4^{2-}	CrO_3F^-	CrO_2F_2	CrO_3Cl^-	CrO_2Cl_2
Cr	1.998 33	1.974 46	1.991 28	1.997 06	2.038 94
O	1.854 96	1.806 92	1.788 60	1.811 02	1.793 16
F		1.879 24	1.856 10		
Cl				2.615 59	2.559 17
outer	4.872 99	5.027 64	4.991 71	6.394 97	6.377 99
α_{out}[b]	0.733 07	0.732 08	0.733 14	0.729 55	0.726 21

[a] 1 bohr = 5.29177×10^{-11} m. [b] Valence-electron weighted average of the atomic values $\alpha_{Cr} = 0.71352$, $\alpha_O = 0.74447$, $\sigma_F = 0.73732$, and $\alpha_{Cl} = 0.72325$.

Results

Chromate. The orbital energies calculated for the ground state of CrO_4^{2-} are given in Table III. The ordering of the occupied levels is the same as that found by Ziegler et al.[9] using the HFS–DVM method, but differs slightly from that obtained by Gubanov et al.[7] using the Xα method with "nonoverlapping" spheres and somewhat different α values and sphere radii. However, both earlier studies and our results yield $1t_1$ as the highest occupied level and 2e as the lowest unoccupied level. The distributions of electronic charge in the valence orbitals, included

---

[†] University of California.
[‡] Research Institute of Scripps Clinic.

(1) Wolfsberg, M.; Helmholtz, J. *J. Chem. Phys.* **1952**, *20*, 837.
(2) Helmholtz, L.; Brennan, H.; Wolfsberg, M. *J. Chem. Phys.* **1955**, *23*, 853.
(3) Dahl, J. P.; Ballhausen, C. J. *Adv. Quantum Chem.* **1968**, *4*, 170.
(4) Ballhausen, C. J.; Gray, H. B. Electronic Structure of Metal Complexes. In *Coordination Chemistry*; Martell, A. E., Ed.; Van Nostrand Reinhold: New York, 1971; Chapter 1.
(5) Johnson, K. H. *Adv. Quantum Chem.* **1973**, *7*, 143.
(6) Hillier, I. H.; Saunders, V. R. *Chem. Phys. Lett.* **1971**, *9*, 219. Connor, J. A.; Hillier, I. H.; Saunders, V. R.; Wood, M. H.; Barber, M. *Mol. Phys.* **1972**, *24*, 497.
(7) Gubanov, V. A.; Weber, J.; Connolly, J. W. D. *J. Chem. Phys.* **1975**, *63*, 1455.

0020-1669/89/1328-2738$01.50/0

Table III. Energies (in Ry)[a] and Distributions of Electronic Charge[b] for the Ground-State Orbitals of CrO_4^{2-}

orbital	energy[c]	charge			
		Cr	O	inter	outer
$7a_1$	-0.0588	0.003	0.008	0.231	0.734
$7t_2$	-0.0928	0.527	0.082	0.077	0.069
2e	-0.2487	0.631	0.066	0.074	0.031
$1t_1$	-0.4893	0.007	0.208	0.130	0.032
$6t_2$	-0.5601	0.038	0.184	0.181	0.043
$6a_1$	-0.6017	0.116	0.198	0.029	0.063
1e	-0.6727	0.290	0.132	0.164	0.019
$5t_2$	-0.7218	0.390	0.142	0.007	0.036
$4t_2$	-1.6047	0.071	0.219	0.038	0.016
$5a_1$	-1.6316	0.052	0.218	0.060	0.016
$3t_2$	-3.6196	0.958	0.011	0.000	0.000
$4a_1$	-5.6128	0.978	0.006	0.000	0.000
$2t_2$	-37.4661		(1s)		
$3a_1$	-37.4661		(1s)		
$1t_2$	-41.6367	(2p)			
$2a_1$	-48.8028	(2s)			
$1a_1$	-428.9378	(1s)			

[a] 1 Ry = 2.179907 × 10^{-18} J. [b] Contribution of each sphere or region to the normalized electronic charge in each valence orbital. Entries in parentheses indicate core orbitals. [c] The orbitals below the gap are filled in the ground state.

in Table III, show that the $1t_1$ level consists essentially of just oxygen partial waves (2p), and thus represents an oxygen lone-pair level.[29] The virtual 2e and $7t_2$ orbitals consist predominantly of chromium character (3d) with the 2e < $7t_2$ energy order in agreement with simple crystal field ideas for 3d orbitals in a tetrahedral environment.

The vertical excitation energies for CrO_4^{2-} predicted by the "unrelaxed" ground-state orbital energies and by spin-restricted (SR) and spin-unrestricted (SU) transition states (TS) and total statistical energies (TE) are compared in Table IV. The SR calculations yield higher excitation energies than the SU calculations, and those from total energies are generally slightly higher than from transition states. Similar trends are evident in other Xα calculations.[30] However, the energy ordering of the lower excitations is constant, and the $1t_1 \rightarrow 2e$ excitation at ≈3.4 eV remains the lowest lying by ≥1 eV in all cases.

The energies in Table IV are averages over the states that result from a given orbital configuration.[9,18-20,30] The $1t_1 \rightarrow 2e$ excitation, for example, yields $^{1,3}T_2$ and $^{1,3}T_1$ states. A SR calculation for this excitation gives an average energy of these states, while SU calculations yield separate average energies of the spin-singlet and spin-triplet states. However, when more than one pair of singlet and triplet states arise from a given configuration, conventional Xα–SW calculations cannot predict the ordering of the states or even with confidence the spin multiplicity of the lowest excited state. Ziegler et al.[9] have evaluated the multiplet energies for the $1t_1 \rightarrow 2e$ excitation in CrO_4^{2-} and find that the four states order $^1T_2 > {}^1T_1 > {}^3T_2 > {}^3T_1$ with a mean energy of 2.90 eV and a total energy spread of ≈0.6 eV. By comparison, Gubanov et al.[7] report 2.86 and 3.18 eV for the $1t_1 \rightarrow 2e$ excitation from unrelaxed orbitals and a SR transition-state calculation, respectively.

The distribution of total electronic charge among the atomic, interatomic, and outer regions is shown in Table V for the SR ground $(1t_1)^6(2e)^0$ and excited $(1t_1)^5(2e)^1$ configurations. As has been previously noted[8,10] and shown by the results in Table V, the $1t_1 \rightarrow 2e$ excitation does not result in a significant buildup of charge on the metal (≤0.1 unit), contrary to expectations based on the ground-state orbitals. This results principally because of a considerable redistribution of charge on excitation among orbitals with large chromium 3d character.

Although CrO_4^{2-} is formally a $3d^0$ complex, the chromium charge calculated in the ground state for each of the occupied $5t_2$ (0.390) and 1e (0.290) orbitals arises predominantly from partial waves with $l = 2$ (3d). This follows directly from symmetry for any e orbital since chromium partial waves with l = 0, 1, and 3 cannot contribute. For $5t_2$, the contributions to the chromium charge are 0.007, 0.379, and 0.004 in the ground state and 0.008, 0.329, and 0.004 following $1t_1 \rightarrow 2e$ excitation for l = 1, 2, and 3, respectively. The total contributions to the chromium charge decrease upon excitation from 0.290 to 0.224 for 1e and from 0.390 to 0.341 for $5t_2$. Hence, the decrease in the chromium charge due to the fully occupied 1e and $5t_2$ orbitals is 4(0.066) + 6(0.049) = 0.558 unit, which largely negates the increase resulting from population of the 2e orbital, 0.689 unit. The chromium charge redistributions upon excitation are much less among the other occupied orbitals.

The only significant differences from the above (nonrelativistic) results arising from the relativistic calculations are the splittings of t_1 and t_2 into $\Gamma_6 + \Gamma_8$ and $\Gamma_7 + \Gamma_8$ in T_d double group,[31] respectively, caused by the spin–orbit interactions. The largest splitting, $\Gamma_8 - \Gamma_7 = 8400$ cm^{-1}, obtains for $3t_2$, which is essentially pure chromium 3p character, explaining its sign and large value. The $1t_1$, $4t_2$, and $6t_2$ orbitals are primarily on the oxygen ligands and have much smaller splittings ($\Gamma_8 - \Gamma_{6(7)}$ = 143–222 cm^{-1}), as expected. The splittings of $5t_2$ (mixture of chromium 3d and oxygen 2p) and $7t_2$ (chromium 3d) are $\Gamma_8 - \Gamma_7$ = −7 and −53 cm^{-1}, respectively. The small magnitude and the reversal in sign of the splitting for $7t_2$ is surprising. In a tetrahedral field, where the d orbitals split with $t_2(\Gamma_7 + \Gamma_8) > e(\Gamma_8)$, spin–orbit interactions at the d orbital center should lead to $\Gamma_8 > \Gamma_7$ for t_2. Since the virtual $7t_2$ and 2e orbitals are largely chromium 3d and order $7t_2$ > 2e, the expectation is that $\Gamma_8 > \Gamma_7$ should obtain for $7t_2$ from the chromium-centered interactions. Perturbation by the nearer of the lower lying orbitals with appreciable chromium character ($6a_1$ and 1e) would only further split the $7t_2$ components in the same direction. The calculated splitting might be anticipated for $5t_2$, since the nearest orbital is 1e at slightly greater energy. The actual interactions are of course more complicated than the preceding simple one-center ideas, since both $5t_2$ and $7t_2$ have significant oxygen character, and presumably some cancellation of various contributions is occurring. In any event, the implication

---

(8) Ziegler, T.; Rauk, A.; Baerends, E. J. *Chem. Phys.* **1976**, *16*, 209.

(9) Ziegler, T.; Rauk, A.; Baerends, E. J. *Theor. Chim. Acta* **1977**, *43*, 261.

(10) Johansen, H.; Rettrup, S. *Chem. Phys.* **1983**, *74*, 77. Johansen, H. *Mol. Phys.* **1983**, *49*, 1209.

(11) Dalhoeven, G. A. M.; Blasse, G. *Chem. Phys. Lett.* **1980**, *76*, 27.

(12) Miller, R. M.; Tinti, D. S. *J. Lumin.* **1986**, *36*, 143.

(13) Miller, R. M.; Tinti, D. S. *Mol. Phys.* **1985**, *56*, 923.

(14) Miller, R. M.; Tinti, D. S. *Chem. Phys. Lett.* **1986**, *130*, 352.

(15) Dunn, T. M.; Francis, A. H. *J. Mol. Spectrosc.* **1968**, *25*, 82. Spoliti, M.; Thirtle, J. H.; Dunn, T. M. *J. Mol. Spectrosc.* **1974**, *52*, 146.

(16) Bondybey, V. E. *Chem. Phys.* **1974**, *18*, 293.

(17) Lasko, C. L.; Miller, R. M.; Tinti, D. S. *Chem. Phys. Lett.* **1986**, *130*, 359.

(18) Slater, J. C. *Quantum Theory of Molecules and Solids*; McGraw-Hill: New York, 1974; Vol. 4.

(19) Connolly, J. W. D. *Semiempirical Methods of Electronic Structure Calculation, Part A: Techniques*; Segal, G. A., Ed.; Plenum: New York, 1977; p 274.

(20) Case, D. A. *Annu. Rev. Phys. Chem.* **1982**, *33*, 151.

(21) Collotti, G.; Conti, L.; Zocchi, M. *Acta Crystallogr.* **1959**, *12*, 416.

(22) Granier, W.; Vilminot, S.; Vidal, J. D.; Cot, L. *J. Fluorine Chem.* **1981**, *19*, 123.

(23) Foster, J. J.; Sterns, M. *J. Cryst. Mol. Struct.* **1974**, *4*, 149.

(24) French, R. J.; Hedberg, L.; Hedberg, K.; Gard, G. L.; Johnson, B. M. *Inorg. Chem.* **1983**, *22*, 892.

(25) Marsden, C. J.; Hedberg, L.; Hedberg, K. *Inorg. Chem.* **1982**, *21*, 1115.

(26) Schwarz, K. *Phys. Rev. B* **1972**, *5*, 2466.

(27) Norman, J. G. *Mol. Phys.* **1976**, *31*, 1191.

(28) Watson, R. E. *Phys. Rev.* **1958**, *111*, 1108.

(29) With l_{max}(Cr) = 2, no amplitude obtains for chromium partial waves in $1t_1$, as follows from symmetry for a minimal basis, but for l_{max}(Cr) = 3, a small amount of chromium character (4f) results.

(30) Messmer, R. P.; Salahub, D. R. *J. Chem. Phys.* **1976**, *65*, 779.

(31) $\Gamma_6 \equiv E_{1/2}$, $\Gamma_7 \equiv E_{5/2}$, $\Gamma_8 \equiv G_{3/2}$; $\Gamma_{1,2} \equiv A_{1,2}$, $\Gamma_3 \equiv E$, $\Gamma_{4,5} \equiv T_{1,2}$ $(F_{1,2})$: Herzberg, G. *Molecular Spectra and Molecular Structure*; Van Nostrand: Princeton, NJ, 1966; Vol. III, Appendix I.

Table IV. Calculated Transition Energies (in eV) for the Lower Excitations of CrO_4^{2-}, CrO_3F^-, CrO_3Cl^-, CrO_2F_2, and CrO_2Cl_2

				SU-TS[d]		SU-TE[e]	
excitation	unrel orbital[a]	SR-TS[b]	SR-TE[c]	trip.	sing.	trip.	sing.
CrO_4^{2-}							
$1t_1 \rightarrow 2e$	3.27	3.66	3.79	3.29	3.31	3.42	3.43
$6t_2 \rightarrow 2e$	4.24	4.59	4.71	4.23	4.34	4.36	4.45
$6a_1 \rightarrow 2e$	4.80	5.11	5.27	4.73	4.90	4.89	5.05
$1t_1 \rightarrow 7t_2$	5.39	5.66	5.60	5.31	5.50	5.31	5.36
CrO_3F^-							
$1a_2 \rightarrow 9e$	3.13	3.52	3.72	3.08	3.17	3.29	3.35
$8e \rightarrow 9e$	3.59	3.94	4.15	3.54	3.66	3.74	3.85
$12a_1 \rightarrow 9e$	4.28	4.62	4.82	4.22	4.38	4.42	4.57
$1a_2 \rightarrow 13a_1$	4.29	4.72	4.88	4.33	4.28	4.49	4.46
$8e \rightarrow 13a_1$	4.75	5.12	5.28	4.75	4.77	4.92	4.94
CrO_3Cl^-							
$1a_2 \rightarrow 10e$	3.00	3.33	3.54	2.90	3.01	3.11	3.19
$9e \rightarrow 10e$	3.30	3.62	3.84	3.25	3.38	3.47	3.58
$10a_2 \rightarrow 15a_1$	3.75	4.13	4.28	3.75	3.73	3.90	3.89
$14a_1 \rightarrow 10e$	4.03	4.32	4.50	3.96	4.12	4.18	4.32
$9e \rightarrow 15a_1$	4.05	4.31	4.55	3.98	4.05	4.17	4.24
CrO_2F_2							
$7b_2 \rightarrow 14a_1$	2.81	3.24	3.43	2.71	2.68	2.91	2.90
$7b_2 \rightarrow 3a_2$	2.98	3.34	3.55	2.77	2.95	2.99	3.18
$7b_1 \rightarrow 14a_1$	3.58	3.90	4.13	3.47	3.55	3.68	3.73
$7b_1 \rightarrow 3a_2$	3.75	4.04	4.27	3.58	3.82	3.78	4.07
$2a_2 \rightarrow 14a_1$	3.84	4.11	4.31	3.69	4.02	3.88	4.21
$2a_2 \rightarrow 3a_2$	4.01	4.28	4.47	3.84	4.29	4.02	4.50
CrO_2Cl_2							
$8b_2 \rightarrow 17a_1$	2.49	2.77	3.02	2.39	2.34	2.61	2.56
$10b_1 \rightarrow 17a_1$	2.51	3.00	3.34	2.69	2.69	3.02	3.04
$3a_2 \rightarrow 17a_1$	2.54	3.04	3.40	2.72	2.76	3.07	3.19
$8b_2 \rightarrow 4a_2$	2.75	3.02	3.29	2.56	2.77	2.80	3.03
$10b_1 \rightarrow 4a_2$	2.77	3.34	3.68	3.03	3.10	3.34	3.51
$3a_2 \rightarrow 4a_2$	2.80	3.40	3.77	3.09	3.18	3.43	3.65

[a] From ground-state orbital energies. [b] From orbital energies of spin-restricted transition states. [c] From spin-restricted total statistical energies. [d] From orbital energies of spin-unrestricted transition states. [e] From spin-unrestricted total statistical energies.

Table V. Total Electronic Charge in Each Region for the Ground and Lowest Excited Configurations of CrO_4^{2-}, CrO_3F^-, CrO_3Cl^-, CrO_2F_2, and CrO_2Cl_2

	charge				
confign[a]	Cr	O	F/Cl	inter	outer
CrO_4^{2-}					
$(1t_1)^6(2e)^0$	22.237	7.949		2.970	0.997
$(1t_1)^5(2e)^1$	22.326	7.923		2.952	1.029
CrO_3F^-					
$(1a_2)^2(9e)^0$	22.235	7.857	8.894	2.754	0.544
$(1a_2)^1(9e)^1$	22.318	7.823	8.905	2.747	0.561
CrO_3Cl^-					
$(1a_2)^2(10e)^0$	22.423	7.888	16.724	3.006	0.183
$(1a_2)^1(10e)^1$	22.495	7.853	16.740	3.010	0.194
CrO_2F_2					
$(7b_2)^2(14a_1)^0$	22.215	7.756	8.822	2.203	0.426
$(7b_2)^1(14a_1)^1$	22.286	7.701	8.833	2.212	0.433
CrO_2Cl_2					
$(8b_2)^2(17a_1)^0$	22.518	7.785	16.554	2.559	0.245
$(8b_2)^1(17a_1)^1$	22.585	7.763	16.534	2.568	0.252

[a] Spin-restricted calculation with all lower energy orbitals fully occupied.

Table VI. Energies (in Ry)[a] and Distributions of Electronic Charge[b] for the Ground-State Orbitals of CrO_3F^-

		charge				
orbital	energy[c]	Cr	O	F	inter	outer
$14a_1$	−0.0572	0.007	0.009	0.008	0.286	0.673
10e	−0.1303	0.519	0.111	0.012	0.098	0.040
$13a_1$	−0.2357	0.600	0.061	0.119	0.069	0.029
9e	−0.3206	0.613	0.089	0.020	0.082	0.018
$1a_2$	−0.5507	0.010	0.278	0.000	0.137	0.018
8e	−0.5847	0.028	0.254	0.030	0.160	0.021
$12a_1$	−0.6355	0.052	0.242	0.020	0.176	0.026
7e	−0.6986	0.162	0.144	0.265	0.124	0.016
$11a_1$	−0.7238	0.152	0.194	0.182	0.052	0.033
6e	−0.7881	0.198	0.076	0.437	0.126	0.012
5e	−0.8364	0.367	0.160	0.118	0.013	0.021
$10a_1$	−0.8466	0.273	0.032	0.592	0.016	0.024
4e	−1.6887	0.098	0.287	0.000	0.032	0.008
$9a_1$	−1.7085	0.074	0.289	0.000	0.051	0.008
$8a_1$	−2.1025	0.021	0.000	0.935	0.036	0.008
$7a_1$	−3.6974	0.969	0.006	0.015	0.000	0.000
3e	−3.7250	0.943	0.019	0.000	0.000	0.000
$6a_1$	−5.7060	0.974	0.008	0.002	0.000	0.000
2e	−37.5523		(1s)			
$5a_1$	−37.5523		(1s)			
1e	−41.7235	(2p)				
$4a_1$	−41.7235	(2p)				
$3a_1$	−48.4766			(1s)		
$2a_1$	−48.8887	(2s)				
$1a_1$	−429.0318	(1s)				

[a–c] See Table III.

of the small splitting of the virtual orbitals is that spin–orbit interactions are not important in a qualitative description of the lower lying excited states.

Halochromates. Tables VI and VII give the ground-state orbital energies and valence orbital charge distributions for CrO_3F^- and CrO_3Cl^-, respectively. On the basis of the results in CrO_4^{2-} and the correlation $t_1(T_d) \rightarrow a_2 + e(C_{3v})$, the highest filled orbitals in CrO_3X^- are anticipated and found to have a_2 and e symmetry. The a_2 orbital has the higher energy, a node at the halogen (not imposed by the basis set for X = Cl), and only slight chromium character. Hence, the highest occupied orbital retains an oxygen lone-pair description. The highest filled e orbital has somewhat greater, although still small, chromium character and a significant halogen contribution (3p) only in CrO_3Cl^-. The latter is expected from, e.g., the relative electronegativities, which should tend to concentrate the fluorine character in lower energy levels. The lowest unoccupied level has e symmetry and predominantly chromium 3d character, as anticipated from the correlation $e(T_d) \rightarrow e(C_{3v})$. Its chromium contribution decreases and its oxygen contribution increases in the order CrO_4^{2-}, CrO_3F^-, CrO_3Cl^-, but

Table VII. Energies (in Ry)[a] and Distributions of Electronic Charge for the Ground-State Orbitals of CrO_3Cl^-

		charge				
orbital	energy[c]	Cr	O	Cl	inter	outer
$16a_1$	−0.0747	0.002	0.006	0.013	0.470	0.496
$11e$	−0.1349	0.522	0.105	0.011	0.125	0.028
$15a_1$	−0.2674	0.553	0.066	0.158	0.071	0.020
$10e$	−0.3226	0.589	0.096	0.017	0.099	0.006
$1a_2$	−0.5430	0.011	0.280	0.000	0.146	0.002
$9e$	−0.5652	0.022	0.205	0.212	0.146	0.006
$14a_1$	−0.6184	0.036	0.202	0.157	0.191	0.010
$8e$	−0.6198	0.018	0.080	0.558	0.171	0.012
$13a_1$	−0.6592	0.120	0.076	0.550	0.077	0.024
$7e$	−0.7257	0.327	0.156	0.057	0.146	0.002
$12a_1$	−0.7763	0.354	0.191	0.046	0.024	0.004
$6e$	−0.8414	0.407	0.195	0.004	0.000	0.002
$11a_1$	−1.4742	0.011	0.000	0.936	0.044	0.007
$5e$	−1.6942	0.109	0.288	0.000	0.026	0.000
$10a_1$	−1.7154	0.085	0.291	0.000	0.041	0.000
$9a_1$	−3.6846	0.976	0.005	0.009	0.000	0.000
$4e$	−3.7256	0.940	0.020	0.000	0.000	0.000
$8a_1$	−5.6998	0.974	0.008	0.002	0.000	0.000
$3e$	−14.0636			(2p)		
$7a_1$	−14.0636			(2p)		
$6a_1$	−18.3599			(2s)		
$2e$	−37.5460		(1s)			
$5a_1$	−37.5460		(1s)			
$1e$	−41.7029	(2p)				
$4a_1$	−41.7029	(2p)				
$3a_1$	−48.8668	(2s)				
$2a_1$	−201.2438			(1s)		
$1a_1$	−429.0234	(1s)				

[a–c] See Table III.

Table VIII. Energies (in Ry)[a] and Distributions of Electronic Charge[b] for the Ground-State Orbitals of CrO_2F_2

		charge				
orbital	energy[c]	Cr	O	F	inter	outer
$16a_1$	−0.0669	0.008	0.009	0.010	0.346	0.608
$8b_2$	−0.2609	0.527	0.161	0.015	0.098	0.023
$15a_1$	−0.3320	0.570	0.116	0.054	0.070	0.020
$8b_1$	−0.4009	0.613	0.062	0.098	0.049	0.016
$3a_2$	−0.4709	0.593	0.142	0.021	0.070	0.010
$14a_1$	−0.4835	0.629	0.100	0.043	0.076	0.010
$7b_2$	−0.6902	0.018	0.406	0.010	0.136	0.014
$7b_1$	−0.7464	0.052	0.306	0.084	0.152	0.015
$2a_2$	−0.7654	0.120	0.204	0.180	0.099	0.011
$13a_1$	−0.8058	0.118	0.242	0.131	0.119	0.016
$6b_1$	−0.8425	0.012	0.013	0.420	0.108	0.014
$6b_2$	−0.8445	0.029	0.045	0.381	0.104	0.015
$12a_1$	−0.8783	0.119	0.174	0.238	0.029	0.029
$11a_1$	−0.9123	0.230	0.079	0.239	0.126	0.008
$1a_2$	−0.9134	0.227	0.074	0.245	0.126	0.008
$5b_1$	−0.9753	0.312	0.022	0.308	0.008	0.020
$10a_1$	−0.9864	0.354	0.127	0.187	0.000	0.018
$5b_2$	−0.9960	0.393	0.260	0.034	0.000	0.017
$4b_2$	−1.8398	0.126	0.430	0.000	0.008	0.006
$9a_1$	−1.8491	0.104	0.433	0.000	0.023	0.006
$4b_1$	−2.2002	0.030	0.000	0.466	0.030	0.007
$8a_1$	−2.2077	0.026	0.000	0.466	0.033	0.007
$3b_1$	−3.8499	0.974	0.001	0.012	0.000	0.000
$7a_1$	−3.8732	0.954	0.018	0.006	0.000	0.000
$3b_2$	−3.8945	0.935	0.032	0.000	0.000	0.000
$6a_1$	−5.8645	0.976	0.009	0.003	0.000	0.000
$2b_2$	−37.7311		(1s)			
$5a_1$	−37.7311		(1s)			
$1b_2$	−41.8887	(2p)				
$2b_1$	−41.8887	(2p)				
$4a_1$	−41.8887	(2p)				
$1b_1$	−48.5914			(1s)		
$3a_1$	−48.5914			(1s)		
$2a_1$	−49.0536	(2s)				
$1a_1$	−429.1996	(1s)				

[a–c] See Table III.

Table IX. Energies (in Ry)[a] and Distributions of Electronic Charge[b] for the Ground-State Orbitals of CrO_2Cl_2

		charge				
orbital	energy[c]	Cr	O	Cl	inter	outer
$19a_1$	−0.0915	0.002	0.007	0.014	0.503	0.452
$9b_2$	−0.2798	0.539	0.149	0.019	0.115	0.010
$18a_1$	−0.3585	0.539	0.117	0.070	0.073	0.014
$11b_1$	−0.4380	0.504	0.072	0.138	0.057	0.019
$4a_2$	−0.4791	0.573	0.151	0.020	0.081	0.003
$17a_1$	−0.4984	0.591	0.094	0.064	0.088	0.006
$8b_2$	−0.6814	0.010	0.260	0.170	0.123	0.006
$10b_1$	−0.6826	0.004	0.055	0.378	0.118	0.012
$3a_2$	−0.6849	0.007	0.063	0.367	0.121	0.012
$16a_1$	−0.7239	0.020	0.043	0.359	0.164	0.012
$7b_2$	−0.7260	0.212	0.163	0.238	0.168	0.008
$9b_1$	−0.7382	0.044	0.166	0.235	0.139	0.016
$15a_1$	−0.7806	0.140	0.039	0.347	0.063	0.025
$8b_1$	−0.8508	0.408	0.117	0.148	0.053	0.009
$2a_2$	−0.8514	0.354	0.212	0.048	0.125	0.001
$14a_1$	−0.8556	0.331	0.249	0.025	0.119	0.001
$13a_1$	−0.9765	0.376	0.299	0.012	0.000	0.002
$6b_2$	−1.0181	0.392	0.299	0.004	0.000	0.002
$7b_1$	−1.5777	0.019	0.000	0.467	0.040	0.007
$12a_1$	−1.5847	0.018	0.000	0.464	0.045	0.007
$5b_2$	−1.8694	0.150	0.425	0.000	0.000	0.000
$11a_1$	−1.8802	0.128	0.435	0.000	0.000	0.000
$6b_1$	−3.8270	0.980	0.001	0.009	0.000	0.000
$10a_1$	−3.8590	0.954	0.019	0.004	0.000	0.000
$4b_2$	−3.8902	0.928	0.036	0.000	0.000	0.000
$9a_1$	−5.8475	0.975	0.010	0.002	0.000	0.000
$3b_2$	−14.1863			(2p)		
$5b_1$	−14.1863			(2p)		
$4b_1$	−14.1863			(2p)		
$1a_2$	−14.1863			(2p)		
$8a_1$	−14.1863			(2p)		
$7a_1$	−14.1863			(2p)		
$3b_1$	−18.4822			(2s)		
$6a_1$	−18.4822			(2s)		
$2b_2$	−37.7517		(1s)			
$5a_1$	−37.7517		(1s)			
$1b_2$	−41.8521	(2p)				
$2b_1$	−41.8521	(2p)				
$4a_1$	−41.8521	(2p)				
$3a_1$	−49.0147	(2s)				
$1b_1$	−201.3689			(1s)		
$2a_1$	−201.3689			(1s)		
$1a_1$	−429.1836	(1s)				

[a–c] See Table III.

the changes are small; the halogen contribution is very small and similar in both halochromates.

The vertical transition energies for CrO_3F^- and CrO_3Cl^- are included in Table IV for the five lowest energy excitations. The $a_2 \rightarrow e$ and $e \rightarrow e$ excitations derived from the parent $1t_1 \rightarrow 2e$ (T_d) excitation have the lowest energies with $a_2 \rightarrow e$ lowest by $\approx$0.4 eV in both anions. The results suggest that the $^{1,3}E$ states arising from $a_2 \rightarrow e$ are the lowest lying excited states with a very small singlet–triplet splitting ($\approx$0.1 eV). However, this prediction disregards the multiplet splitting among the nearby states arising from the $e \rightarrow e$ excitation ($^{1,3}A_1 + {}^{1,3}A_2 + {}^{1,3}E$).

Chromyl Halides. The ground-state orbital energies and the charge distributions in the valence orbitals for CrO_2F_2 and CrO_2Cl_2 are given in Tables VIII and IX, respectively, and follow generally the anticipated trends from the earlier results. The highest filled orbitals derive from the correlation $t_1(T_d) \rightarrow a_2 + b_1 + b_2(C_{2v})$ and have a relative energy ordering $b_2 > b_1 > a_2$ and only slight chromium character. Among these, the b_2 has the greatest oxygen amplitude and the least halogen amplitude, so that the highest occupied orbital is still mainly an oxygen lone-pair level. The halogen character increases in b_1 and a_2 and is considerably larger in CrO_2Cl_2 than in CrO_2F_2, showing the same trend as in CrO_3X^-. The two lowest unfilled orbitals have symmetries a_1 and a_2 with the former being lower lying and are mainly of chromium 3d character. This again follows from the correlation $e(T_d) \rightarrow a_1 + a_2(C_{2v})$. The a_1 orbital has the greater chromium and halogen

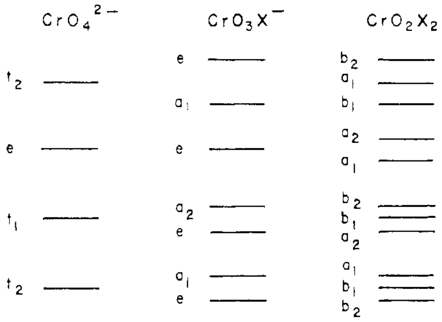

Figure 1. Schematic energy level diagram for the higher filled and lower unfilled orbitals in the ground states of CrO_4^{2-} (T_d), CrO_3X^- (C_{3v}) and CrO_2X_2 (C_{2v}) where X = F and Cl. Orbitals below the gap are filled in the ground state, and the lowest energy excitation is $t_1 \rightarrow e$ in CrO_4^{2-}, $a_2 \rightarrow e$ in CrO_3X^-, and $b_2 \rightarrow a_1$ in CrO_2X_2. The lowest lying orbitals of b_1 and b_2 symmetry in CrO_2X_2 have the order shown for X = F but the opposite order for X = Cl. The C_{2v} axes in CrO_2X_2 have CrX_2 in the *xz* plane and CrO_2 in the *yz* plane.

character and smaller oxygen character than the a_2 orbital. Our results for the energy ordering of the orbitals that derive from $1t_1$ and $2e$ (T_d) differ from the previously reported $X\alpha$ results of Jasinski et al.[32] in these molecules. Jasinski et al. used somewhat different α values, "nonoverlapping" spheres and older geometries. In particular, the geometry of CrO_2F_2 is changed significantly in the newer electron diffraction results.[24]

Table IV includes the vertical transition energies in CrO_2F_2 and CrO_2Cl_2 for the six lowest energy excitations deriving from the parent $1t_1 \rightarrow 2e$ excitation. These correspond to the six lowest energy transitions in CrO_2Cl_2, but several excitations derived from $6t_2 \rightarrow 2e$ and $1t_1 \rightarrow 7t_2$ are nearby (0.3–0.6 eV). However, in CrO_2F_2, the $7b_2 \rightarrow 8b_1$ excitation deriving from $1t_1 \rightarrow 7t_2$ has a lower transition energy than $2a_2 \rightarrow 3a_2$ from $1t_1 \rightarrow 2e$ (by $\approx$0.1 eV). The calculated lowest energy states by $\approx$0.3 eV are $^{1,3}B_2$, obtaining from $7b_2 \rightarrow 14a_1$ and $8b_2 \rightarrow 17a_1$ in CrO_2F_2 and CrO_2Cl_2, respectively. The calculations yield a lower energy for the $^1B_2$ than the $^3B_2$ state by $\approx$0.05 eV for reasons that are unclear.[33] The important point, however, is that the $^{1,3}B_2$ states are calculationally nearly degenerate.

Discussion

The generally accepted assignment for the lowest energy excitation in tetraoxo complexes of closed-shell transition metals is the nominal "charge transfer" from ligand to metal, $t_1 \rightarrow e$, leading to $^{1,3}T_1$ and $^{1,3}T_2$ states. There is also general agreement that the dipole-forbidden $^1T_1$ state lies lower than the dipole-allowed $^1T_2$ state for both CrO_4^{2-} and MnO_4^-. The ordering of the triplet states is much less certain. Calculations yield $^1T_2 > {}^1T_1 > {}^3T_2 > {}^3T_1$ for CrO_4^{2-}, but $^1T_2 > {}^1T_1 > {}^3T_1 > {}^3T_2$ for MnO_4^-, with a total spread of $\approx$0.6 eV and a splitting between the $^1T_1$ and the lowest spin-triplet state of only $\approx$0.1 eV.[9,10] Phosphorescence has been observed from certain CrO_4^{2-} salts at low temperatures,[11,12] showing that a triplet state does lie just below the lowest excited singlet state, but the experimental results also show that the triplet state has less than T_d symmetry so that crystal field and/or Jahn–Teller effects are operative.[12]

Table X. Comparison of Calculated and Experimental Energies (in eV) for the Lowest Energy Transitions

		energy			
		SU-TS[a]	SU-TE[a]	expt[b]	ref
CrO_4^{2-}	$1t_1 \rightarrow 2e$	3.3	3.4	3.1, 3.4	40
CrO_3F^-	$1a_2 \rightarrow 9e$	3.1	3.3	2.8	41
CrO_3Cl^-	$1a_2 \rightarrow 10e$	2.9	3.1	2.8	41
CrO_2F_2	$7b_2 \rightarrow 14a_1$	2.7	2.9	2.6	32
CrO_2Cl_2	$8b_2 \rightarrow 17a_1$	2.3	2.6	2.4	32

[a] Mean of singlet and triplet energies from SU–TS and SU–TE results of Table IV. [b] Lowest energy maximum of absorption spectrum. For CrO_4^{2-}, the two lowest energy maxima are given since the excitation yields T_1 and T_2 states.

The lowest energy excitations in CrO_3X^- and CrO_2X_2 derive from the parent $1t_1 \rightarrow 2e$ excitation. The calculated relative ordering of the relevant orbitals is shown in Figure 1. The lowest virtual and highest filled orbitals remain largely of chromium 3d and oxygen lone-pair character, respectively. Significant halogen contribution in the higher filled orbitals occurs only in CrO_2Cl_2. Neglecting multiplet splitting of the $e \rightarrow e$ excitation in CrO_3X^- and configuration interaction in CrO_3X^- and CrO_2X_2, the lowest excited states are predicted to be $^{1,3}E$ from $a_2 \rightarrow e$ in CrO_3X^- and $^{1,3}B_2$ from $b_2 \rightarrow a_1$ in CrO_2X_2 for X = F and Cl. The singlet–triplet splittings of these states estimated from the SU calculations are small ($\leq$0.1 eV) in all cases. These states are only qualitatively oxygen to chromium charge transfers, since, as in CrO_4^{2-}, considerable reorganization of the charge distribution occurs on excitation so that little charge actually transfers to chromium. Table V includes the total charge distributions for the ground and the above excited configurations of CrO_3X^- and CrO_2X_2.

The available experimental data in CrO_3X^- and CrO_2X_2 are in satisfactory agreement with the above predictions. The lowest excited singlet state in $KCrO_3Cl$ has been assigned as deriving from ^1E based on an observed *xy* polarization in absorption.[34] The lowest triplet state of CrO_3Cl^- lies only $\approx$0.06 eV lower than the onset of the lowest excited singlet state in its K^+, Rb^+, and Cs^+ salts.[13,14] The fine structure splittings and orientation of the spin axes in the triplet state and the vibronic structure of the phosphorescence spectra[13,14,35] show that the triplet state deviates considerably from C_{3v} symmetry, not inconsistent with a Jahn–Teller distortion of a ^3E state promoted by e modes. The experimental data for CrO_3F^- are more limited. However, the lowest lying excited states are again a very close-lying singlet–triplet pair.[13]

The lowest excited singlet states of CrO_2F_2[36] and CrO_2Cl_2[37] have been assigned from rotational analysis as $^1B_2$ (accounting for a change of axes from the rotational system). The lowest triplet state of CrO_2Cl_2 has been observed in various solid hosts at $\leq$0.03 eV below the lowest excited singlet state,[15-17] and presumably corresponds to the $^3B_2$ state. The photophysics of the $^{1,3}B_2$ states of CrO_2Cl_2 manifest various enigmas,[37-39] which may relate to interactions among these states and the several others calculated to lie within 0.5 eV. Rotational perturbations are in fact seen in the $^1B_2$ state of CrO_2F_2.[36]

The experimental energies of the above states are compared with the calculated energies in Table X. The agreement is judged reasonable considering the approximations in the calculations. The experimental Franck–Condon envelopes are also rather wide in these systems, implying significant geometry changes in the excited

---

(32) Jasinski, J. P.; Holt, S. L.; Wood, J. H.; Asprey, L. B. *J. Chem. Phys.* **1975**, *63*, 757.

(33) For the cases considered in Table IV, the triplet energy is greater than the singlet energy only for the excitations $b_2 \rightarrow a_1$ in CrO_2X_2 and $a_2 \rightarrow a_1$ in CrO_3X^-. Both the transition state and total statistical energy methods, used to estimate the separate energies of the singlet and triplet states, yield this result with nearly identical singlet–triplet splittings. The sensitivity to the muffin-tin model was investigated for the $b_2 \rightarrow a_1$ excitation of CrO_2Cl_2 by changing the radius of the chromium sphere with the other radii held constant. The singlet and triplet energies from SU-TE calculations are roughly proportional to the chromium radius for small changes about the Norman value ($\pm$0.1 bohr) with a slope of $\approx$1.2 eV/bohr, but the triplet energy remains greater than the singlet energy by $\approx$0.05 eV. Hence, the muffin-tin approximation does not appear to be the primary cause of the anomalous singlet–triplet ordering. Another possible problem source is the use of "average" orbitals to extract the singlet energy.

(34) Hog, J. H.; Ballhausen, C. J.; Solomon, E. I. *Mol. Phys.* **1976**, *32*, 807.

(35) Miller, R. M.; Tinti, D. S. To be submitted for publication.

(36) Beattie, I. R.; Brown, J. B.; Firth, S.; Gordon, R. D.; Gilson, T. R.; Jones, P. J.; Levy, M. R.; Millington, K. R.; Williams, S. J. *Chem. Phys. Lett.* **1984**, *108*, 138. Gordon, R. D.; Beattie, I. R.; Brown, J. M.; Firth, S. *J. Chem. Phys.* **1986**, *85*, 2423.

(37) Blazy, J. A.; Levy, D. H. *J. Chem. Phys.* **1978**, *69*, 2901.

(38) Mc Donald, J. R. *Chem. Phys.* **1975**, *9*, 423.

(39) Tinti, D. S.; Baskin, J. S.; Zewail, A. H. *Chem. Phys. Lett.* **1989**, *155*, 243.

(40) Johnson, L. W.; McGlynn, S. P. *Chem. Phys. Lett.* **1970**, *7*, 618. Duinker, J. C.; Ballhausen, C. J. *Theor. Chim. Acta* **1968**, *12*, 325.

(41) Miskowski, V.; Gray, H. B.; Ballhausen, C. J. *Mol. Phys.* **1974**, *28*, 729.

states, whereas the calculations refer to vertical energies based on the ground-state geometries. The calculations correctly account for the observed blue shift of the lowest energy singlet state of CrO_2F_2 relative to that of CrO_2Cl_2. A similar shift calculated for CrO_3X^- is not apparent in the experimental data.

Acknowledgment. This work was supported in part by a grant from the National Science Foundation.

Registry No. CrO_4^{2-}, 13907-45-4; CrO_3F^-, 17185-83-0; CrO_3Cl^-, 15906-70-4; CrO_2F_2, 7788-96-7; CrO_2Cl_2, 14977-61-8.

Contribution from the Department of Chemistry and Materials Science Center,
Cornell University, Ithaca, New York 14853

Electronic Structure of One-Dimensional Linear Halogen-Bridged Gold Chains

Christoph Janiak and Roald Hoffmann*

Received January 27, 1989

The band structures of linear halogen-bridged mixed-valent gold chains of the form $\{Au^{III}X_2L_2\text{–}Au^{I}L_2\}_\infty$ (X = bridging Cl, Br; L = terminal-ligand SH_2, Cl, and/or H) were studied by using the extended Hückel method. The valence band was found to be a ligand lone-pair combination—a result unexpected from studies on analogous platinum chains. The variation of the band gap as a function of different geometries is in agreement with experimental results.

Introduction

Halogen-bridged one-dimensional metal complexes show interesting optical properties. Mixed-valence Pt^{II}/Pt^{IV} complexes containing $\cdots X\text{–}Pt^{IV}L_4\text{–}X\cdots Pt^{II}L_4\cdots$ linear chains (X = halogen, L = amine ligand) are the best known and extensively studied examples of these low-dimensional compounds.[1-3] Recent investigations on one-dimensional halogen-bridged complexes include X-ray structural studies[4-10] and Raman, resonance-Raman,[9-14] and electronic[9-18] spectroscopy. A perceptive theoretical analysis of the halogen-bridged platinum chains was carried out by Whangbo and Foshee.[19] A more general approach to linear M–X–M linkages in molecules, polymers, and extended networks was undertaken by Wheeler et al.[20]

Only a small number—albeit increasing—of halogen-bridged linear chains involving metals other than platinum, such as palladium,[3,6,8,13,15,21] nickel,[3,5,6,12,22] copper,[4] and gold are known. Compared to those of their platinum analogues, studies of the one-dimensional gold complexes, for instance $\{Au^{III}X_3(DBS)\text{–}Au^{I}X(DBS)\}_\infty$ (X = Cl, Br; DBS = dibenzyl sulfide, $S(CH_2C_6H_5)_2$), are scarce,[23-25] although their syntheses[26,27] and solid-state structure[23] were established quite early.

This paper is concerned with the differences and similarities in the electronic structures of the one-dimensional Au and Pt complexes.[19] Our work was stimulated by a recent paper by Tanino et al.[25]

Results and Discussion

According to a recent single-crystal X-ray structural investigation, $AuCl_2(DBS)$ consists of alternating $Au^{III}Cl_3(DBS)$ and $Au^{I}Cl(DBS)$ units in a neutral, almost linear chain, shown schematically in **1**.[25,28]

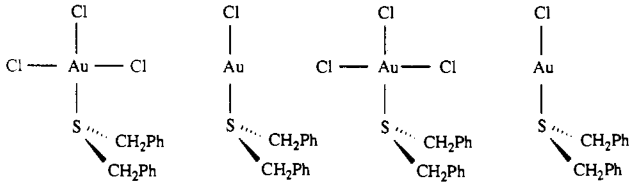

1

Different chains slip in random fashion, owing to a weak three-dimensional correlation (disorder perpendicular to the chains), to give two statistically half-occupied halide positions: Thus, the bridging chlorines appear disordered in the crystal

---

(1) Day, P. In *Low-Dimensional Cooperative Phenomena*; Keller, H. J., Ed.; Plenum Press: New York, 1975; p 191.

(2) Keller, H. J. In *Extended Linear Chain Compounds*; Miller, J. S., Ed.; Plenum Press: New York, 1982; Vol. 1, p 357.

(3) Clark, R. J. H. In *Advances in Infrared and Raman Spectroscopy*; Clark, R. J. H., Hester, R. E., Eds.; Wiley: New York, 1984; Vol. 11, p 95.

(4) Oshio, H.; Toriumi, K.; Bando, S. *Chem. Lett.* **1988**, 1713.

(5) Evans, J.; Gauntlett, J. T.; Levason, W. *Inorg. Chem.* **1988**, *27*, 4521.

(6) Toriumi, K.; Yamashita, M.; Murase, I. *Chem. Lett.* **1986**, 1753.

(7) Tanaka, M.; Tsujikawa, I.; Toriumi, K.; Ito, T. *Acta Crystallogr.* **1986**, *C42*, 1105.

(8) Toriumi, K.; Yamashita, M.; Ito, H.; Ito, T. *Acta Crystallogr.* **1986**, *C42*, 963.

(9) Fanizzi, F. P.; Natile, G.; Lanfranchi, M.; Tiripicchio, A.; Clark, R. J. H.; Kurmoo, M. *J. Chem. Soc., Dalton Trans.* **1986**, 273.

(10) Clark, R. J. H.; Croud, V. B.; Dawes, H. M.; Hursthouse, M. B. *J. Chem. Soc., Dalton Trans.* **1986**, 403.

(11) Clark, R. J. H.; Croud, V. B.; Khokhar, A. R. *Inorg. Chem.* **1987**, *26*, 3284.

(12) Clark, R. J. H.; Croud, V. B. *Inorg. Chem.* **1986**, *25*, 1751.

(13) Clark, R. J. H.; Croud, V. B.; Kurmoo, M. *J. Chem. Soc., Dalton Trans.* **1985**, 815.

(14) Clark, R. J. H.; Kurmoo, M. *J. Chem. Soc., Dalton Trans.* **1985**, 579.

(15) Wada, Y.; Mitani, T.; Yamashita, M.; Koda, T. *J. Phys. Soc. Jpn.* **1985**, *54*, 3143.

(16) Tanaka, M.; Kurita, S.; Fujisawa, M.; Matsumoto, S. *J. Phys. Soc. Jpn.* **1985**, *54*, 3632.

(17) Wada, Y.; Mitani, T.; Yamashita, M.; Koda, T. *Synth. Met.* **1987**, *19*, 907.

(18) Tanaka, M.; Kaneko, W.; Kurita, S.; Yamada, A.; Fukutani, H. *J. Phys. Soc. Jpn.* **1987**, *56*, 1197.

(19) Whangbo, M.-H.; Foshee, M. J. *Inorg. Chem.* **1981**, *20*, 113.

(20) Wheeler, R. A.; Whangbo, M.-H.; Hughbanks, T.; Hoffmann, R.; Burdett, J. K.; Albright, T. A. *J. Am. Chem. Soc.* **1986**, *108*, 2222. See also: Burdett, J. K. *Inorg. Chem.* **1978**, *17*, 2537. Lauher, J. W. *Inorg. Chem.* **1980**, *39*, 119. Burdett, J. K. *Comments Inorg. Chem.* **1981**, *1*, 85.

(21) Clark, R. J. H.; Croud, V. B.; Kurmoo, M. *Inorg. Chem.* **1984**, *23*, 2499.

(22) Cooper, D. A.; Higgins, S. J.; Levason, W. *J. Chem. Soc., Dalton Trans.* **1983**, 2131.

(23) Brain, F. H.; Gibson, C. S.; Jarvis, J. A. J.; Phillips, R. F.; Powell, H. M.; Tyabji, A. *J. Chem. Soc.* **1952**, 3686.

(24) Interrante, L. V.; Bundy, F. P. *J. Inorg. Nucl. Chem.* **1977**, *39*, 1333.

(25) Tanino, H.; Takahashi, K.; Tajima, M.; Kato, M.; Yao, T. *Phys. Rev.* **1988**, *B38*, 8327.

(26) Herrmann, F. *Ber. Dtsch. Chem. Ges.* **1905**, *38*, 2813.

(27) Smith, G. M. *J. Am. Chem. Soc.* **1922**, *44*, 1769.

(28) Takahashi, K.; Tanino, H. *Chem. Lett.* **1988**, 641.

0020-1669/89/1328-2743$01.50/0